Discover Applied Sciences

Research

Geoinformatics and AHP multi criteria decision making integrated flood hazard zone mapping over Modjo catchment, Awash river basin, central Ethiopia

Bereket Abera Bedada[1] · **Wakjira Takala Dibaba**[1]

Received: 10 October 2024 / Accepted: 3 March 2025
Published online: 31 March 2025

Abstract
Flood hazards are natural disasters that profoundly influence the environment and society. To effectively control the incidence of flooding, it is crucial to identify and map regions susceptible to flooding. The Modjo catchment is frequently hampered by flooding, making it crucial to map and identify flood hazard zones. This study aimed to identify and locate the flood hazard zones of the Modjo catchment employing the integrated use of multi-criteria decision-making and geoinformatics tools. Ten influencing factors were used to develop flood hazard zones: drainage density, curvature, rainfall, distance from the river, soil type, elevation, slope, topographic wetness index, land use/cover, and the normalized difference vegetation index. Subsequently, raster-formatted thematic layers of these influencing elements were created, and appropriate weighting was assigned based on their relative responses to the occurrence of flood events and overlayed using the overlay GIS spatial analysis tool. The flood hazard potential zone in the study area was generated and classified into five groups: negligible, low, intermediate, high, and severe. According to the results, the negligible, low, intermediate, high, and severe zones were represented by 0.686% (9.74 km^2), 16.73516% (237.5649 km^2) 74.12% (1052.28 km^2), 8.44% (119.94 km^2), and 0.0012% (0.018 km^2), respectively. The weighting and ranking processes are well reflected in the final flood hazard zone map. The results revealed that a substantial area of the catchment is at risk. Ultimately, 29 observed flood datasets were used to confirm the outcome, yielding an accuracy of > 75% and an area under the ROC curve of 0.868. Most of the flood point data were found in high and severe regions. Considering the verified results, relevant organizations should participate in creating sustainable management plans.

Highlights

- Integrating MCDM with GIS analysis enables precise flood hazard mapping, essential for smart climate resilient urban planning.
- The findings revealed that a significant portion of the catchment highlights a striking concentration of very high and high flood hazard zones.
- It is crucial to implement mitigation measures and disaster preparedness in critical hazard zones within the catchment.

Keywords Flood · Geoinformatics · MCDM · Modjo · Spatial analysis · And sustainability

✉ Bereket Abera Bedada, bereket.abera2028@gmail.com; Wakjira Takala Dibaba, wakjira.takala@ju.edu.et | [1]Faculty of Civil and Environmental Engineering, Jimma University, P.O. Box. 378, Jimma, Ethiopia.

1 Introduction

The impact of natural disasters poses substantial danger to global socioeconomic stability and the environment. The term natural hazard refers to the natural events that possess the capacity to affect societies and environments. In the last 20 years, natural disasters have claimed at least 3 million people globally and negatively impacted around 800 million people [1], and anticipated annual economic losses range from 260 to 310 billion dollars [2]. Natural disasters were responsible for 15,082 fatalities, 100 million displaced people, and an estimated 190 billion US dollars in global economic losses in 2020 year [3]. Vast ranges of events are classified as natural hazards, including landslides, earthquakes, flooding, storms, droughts, wildfires, and eruptions of volcanoes. [4]. All of these events have the potential to seriously harm infrastructure, human lives, and the environment.

Among the many different kinds of natural disasters, floods are particularly dangerous and cause massive damage all over the world [5–9] resulting in substantial economic losses [10], destruction of infrastructure [11], detrimental effects on livelihood [12], biodiversity [13], and serious safety and health risks [14], all of which can lead to cascading impacts across multiple sectors and communities. From 1975, there have occurred annual decreases of about 6 fatalities and over 30,000 people impacted by each occurrence [15]. Cities in the global south are far more vulnerable to natural disasters like floods than cities in the global north due to their severe destitution, rapid growth in population, uncontrolled settlements, degraded surroundings, and weak administration [16]. In Africa, floods are a serious environmental threat that have claimed nearly 27,000 lives between 1950 and 2019 [17]. Among all, East Africa is known for its concurrent flood occurrence, and as a center for eastern Africa Ethiopia is typical example for this regard.

Ethiopia faces a serious problem with flooding, which has been made worse by periods of heavy precipitation that have resulted in significant damage of life and property [18]. Nowadays, the occurrence and causes of flood risks are increasing from time to time as a result of new developments and human settlements on flood-prone areas with major observation in Awash river basin [19]. The Awash Basin in Ethiopia experiences frequent flooding, sometimes with devastating consequences [20]. Flooding has been a significant problem in the upper awash river basin, impacting thousands of individuals and leading to substantial economic losses [21]. Rainfall variability in the Modjo catchment significantly influences the region's vulnerability to flooding. The area's unpredictable rainfall patterns, marked by irregular distributions and intensities, can lead to sudden surges in river flow [22]. Flooding in the Modjo catchment is primarily caused by river overflow, low-lying areas, intense rainfall, and other contributing factors such as land use changes and drainage obstructions. Tracking and locating places at danger of flooding For disaster management and mitigation plans to be successful and long-lasting, flash flood control techniques must be updated [23]. A variety of soft computing techniques, statistical techniques, physically based hydrological models, and multi-criteria decision-making (MCDM) techniques are employed to assess flood susceptibility [24]. Existing flood projection methods frequently suffer from issues including poor resolution, out-of-date data, and the incapacity to take quickly changing environmental variables into account. As a result, flood hazard assessments and mitigation efforts may be erroneous. Scholars are using MCDM methods more frequently because they are efficient at handling complicated decisions with several competing standards, which makes it possible to evaluate options more thoroughly and improves the effectiveness of decisions in a variety of sectors. A decision-making technique called MCDM was created to offer remedies and mitigating actions for complex decision-making issues [25]. A geographic information system (GIS) multicriteria decision support framework for flood vulnerability assessments can be created by integrating multicriteria decision analysis (MCDA) with the GIS [26]. It is possible to map flood hazard efficiently, affordably, and promptly by combining the use of MCDA and GIS in an integrated manner, which saves money, time, and resources. The successful integration of GIS and MCDA during the last few years has been employed frequently in risk evaluation and the creation of flood risk maps, according to numerous studies [27]. Among the most commonly used techniques for MCDM is the analytical hierarchy process (AHP) [28]. The international scientific community has acknowledged the GIS-AHP incorporated technique as an immensely beneficial instrument because of its capacity to handle challenging issues and provide appropriate conclusions [29, 30]. The AHP and GIS method for flood hazard mapping is advantageous due to its ability to integrate diverse data sources for comprehensive analysis, its applicability across various geographic contexts, its flexibility in adjusting criteria based on specific local conditions, and its user-friendly interface that simplifies the mapping process for effective decision-making. The theoretical soundness and practical efficacy of AHP have also been extensively studied [31]. Despite their advantages, AHP and GIS analysis for flood hazard mapping are limited as, every methods have, by the subjective weighting of criteria, which can introduce bias and affect result consistency. Moreover, integrating diverse data sources can lead to inaccuracies if data quality or

spatial resolution is insufficient, making it essential to consider these limitations and shortcomings in the analysis. The reliance on subjective judgments can introduce bias, affecting the consistency and reliability of the results.

The study was carried out in the Modjo catchment of the Awash River basin, located in the Oromia Regional State of Ethiopia. The Modjo watershed is situated in the upper Awash River basin, where frequent floods have a severe negative influence on the surrounding ecosystems and inhabitants [18]. Preparedness for disaster management will be extremely difficult in this area since it has been determined to be notably sensitive to flooding, which will be made worse by climate change and fluctuating rainfall patterns [32]. The main objective of the present study is to identify and visually represent the flood hazard zone through the integrated use of MCDM and geoinformatics tools. This study took into account thematic layers of flood susceptibility causing characteristics such as distance from the river, normalized difference vegetation index (NDVI), drainage density, curvature, rainfall, soil type, elevation, slope, topographic wetness index (TWI), and land use/land cover (LULC) for the potential zone. These factors are crucial for pinpointing locations with a higher hazard of flooding. The weights were distributed based on the experts' recommendations, site characteristics, and response to the likelihood of flood events. Thematic layers were combined using GIS map algebra tool following the AHP method and rank assignment to produce the flood susceptibility zones map. The thematic layers and final generated study flood hazard zone map was categorized into five groups: negligible, low, intermediate, high and sever. The findings of the study were cross validated with observed flood points, and statistically and visually represented using Receiver operative chrematistics (ROC) curve and GIS mapping.

2 Data and methods

2.1 Study area

The study was carried out in the Modjo catchment of the Awash River basin, located in the Oromia Regional State of Ethiopia. Its absolute location is between Latitudes: 8°40′ to 9°4′N; and longitudes: 39°56′ to 39°13′E as shown in Fig. 1. The area coverage is approximately 1419.55 square kilometers. The catchment is characterized by undulating topography, deep and wide valleys of small streams, and narrow flat lands in the southern part caused by poor land-use practices, soil erosion, and deposition processes. In the research area, the catchment and its tributaries provide a continual supply of water to the Modjo River, with a total annual mean flow of 214.55 m^3/s. The catchment elevation runs between 1764 and 3091 m. The catchment receives an average annual rainfall of 427 mm, ranging from 387 mm to a maximum of 511 mm. The mean minimum and mean maximum monthly temperature of the area varies from 9.96 °C to 18.76 °C and 26.8 °C to 35.70 °C, respectively. The maximum temperature in this catchment is in May, and the minimum temperature in this study area occurs in December. June to September is the main rainy season in the catchment, and a peak occurs between July and August. The methodology used in this study is illustrated in Fig. 2.

2.2 Data description

The weighted overlay analysis is a data-intensive manipulation, and to achieve the required main objective and quality results, gathering and providing accurate data to the GIS workspace is mandatory. High-resolution satellite data were used along with field data such as observed rainfall. Observed flood occurrence point data was used for result validation, and obtained from the two-year observation and experience in the catchment. Table 1 displays an overview of all the data that was utilized. All data sets have their own limitations. FAO soil maps are typically created using conceptual soil and landscape knowledge, which can vary among surveyors. These maps aggregate data over large areas, lacking the ability to provide precise, location-specific details about soil properties. CHIRPS data may be prone to errors in precipitation estimates, particularly in regions with few weather stations. Esri Land Cover data can experience classification mistakes due to cloud cover and infrequent updates, while Landsat data is limited by its 1 potential atmospheric disturbances that can obscure land surface features. This study recognizes these limitations and works to reduce the inaccuracies caused by them.

The objective of this study is to determine probable flood hazard zones in the Modjo catchment's different topographical conditions using an inexpensive interdisciplinary research strategy that integrates the GIS and the AHP-MCDM technique. Selecting flood-causing elements, calculating weights using AHP, creating a spatial database, and validating the generated flood hazard zone map using flood inventory data were the four processes involved in creating prospective flood hazard zones. ArcGIS 10.8 software was used to construct all of the thematic maps in

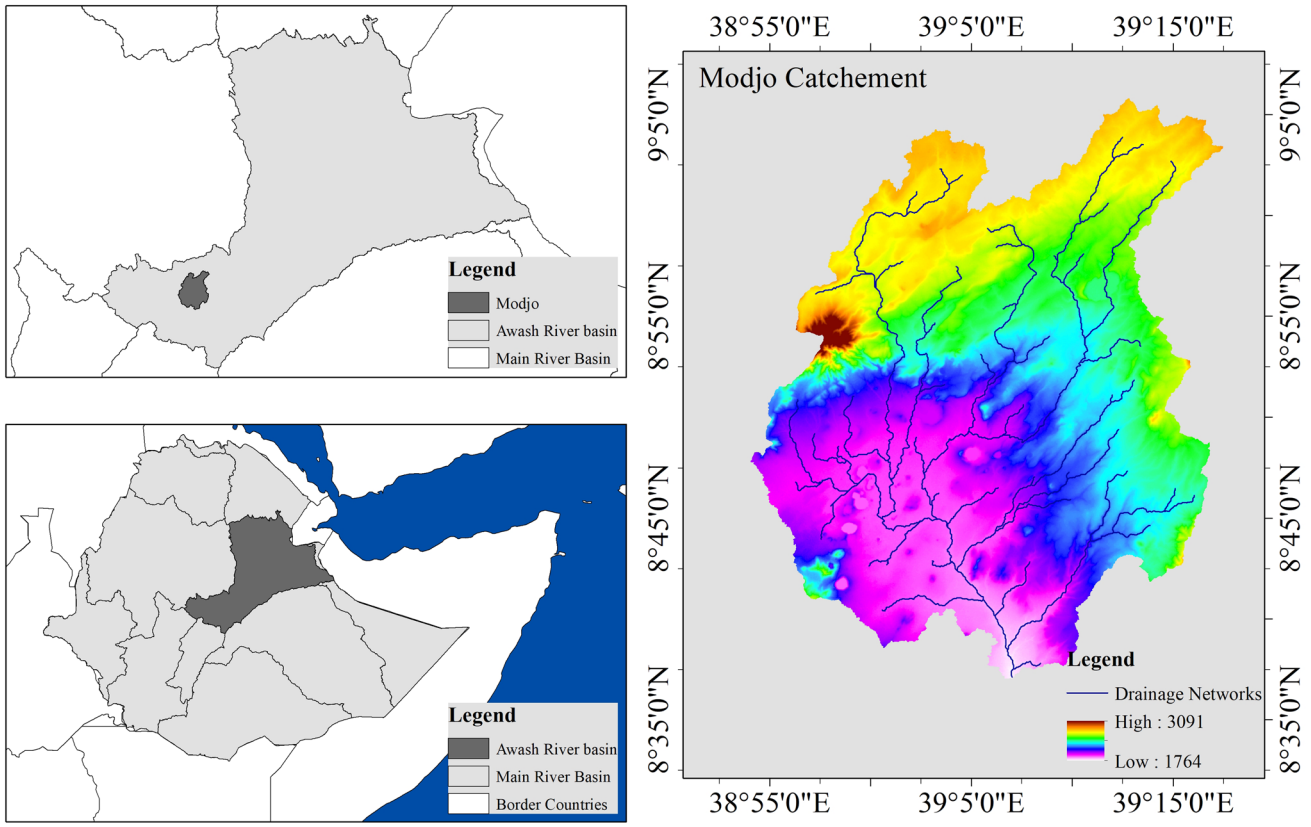

Fig. 1 Map of the study area

raster format using remote sensing data. Produced thematic maps included curvature, drainage density, TWI, distance from the river, LULC, slope, soil type, rainfall, NDVI, and elevation. The thematic layers were projected with the WGS84/UTM Zone 37 N datum coordinate system in a resampled resolution of 30 × 30 m. All data were integrated and examined in a GIS to assess the flood event controlling features. Finally, flood hazard zone maps were prepared based on the GIS overlay analysis.

2.3 Thematic layers

The selection and relative importance of thematic layers in flood hazard mapping were determined by analyzing previous studies, consulting expert opinions, and considering the actual conditions of the site. This comprehensive approach ensures that the mapping process is grounded in established research and practical insights, leading to more accurate and effective flood risk assessments.

2.3.1 Rainfall

Rainfall is not only the primary source of surface and groundwater recharge because it enables water to seep through soils and cracks beneath the surface, but it also plays a significant role in determining the likelihood of flooding in areas [33]. The rainfall map of the study area was extracted from average 5 year annual precipitation data received from ten meteorological stations located in the catchment and was substantially sourced adjacent to it, and interpolated using the inverse distance weighting (IDW) method. Floods are directly correlated with rainfall; the likelihood of a flood probability usually rises with increasing precipitation. A weight of 0.15 has been assigned to the rainfall thematic layer.

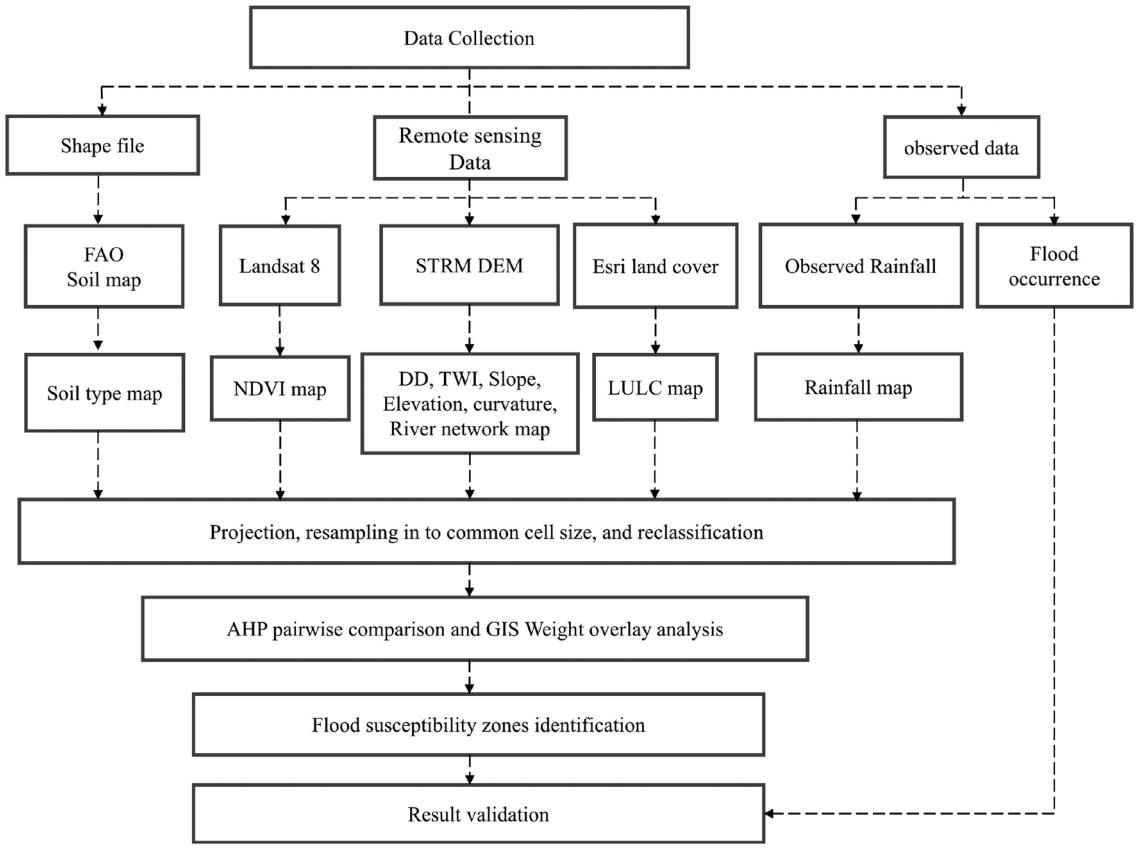

Fig. 2 Methodology flowchart

Table 1 Data used in the study

Data type	Source	Date of acquisition	Spatial resolution	Output layer
Rainfall	CHIRPS	21/06/2024	Point data	Rainfall map
Landsat 8	USGS	19/07/2024	30 m × 30 m	NDVI map
Soil map	FAO	21/07/2024		Soil type map
STRM DEM	USGS	24/07/2024	30 m × 30 m	Elevation, Slope, drainage density, TWI, Curvature, and distance from the river map
Sentinel 2 land cover	Esri	18/07/2024	10 m	Land use/cover map
Flood occurrence	Observation	21/10/2023	Point data	Result validation

2.3.2 Drainage density

One of the main factors influencing food dangers is drainage density. Drainage density has a substantial impact on concentration time, which in turn influences the magnitude of peak flow during flooding events [34]. The potential for streamflow is shown by drainage density, which is the ratio of the total drainage length per unit area [35]. The drainage is controlled by the nature, structure, and lithology of the bedrock, the soil's capacity to infiltrate, the type of vegetation, and the slope angle [36]. There is an inverse relationship between drainage density and permeability [37]. Typically, flood occurrence is directly proportional to drainage density; a high drainage density leads to a major flood hazard susceptibility zone, whereas a low density leads to a relatively low flood hazard susceptibility zone. Drainage density values of the catchment were calculated from DEM raster data on the ArcGIS workspace using a spatial analysis tool. A weight of 0.07 has been assigned to the Drainage density thematic layer.

2.3.3 Soil type

Soil type plays a critical role in flood occurrence by influencing water absorption, retention capacity, and drainage characteristics, with sandy soils facilitating quicker drainage and clay soils retaining water, thereby increasing the risk of flooding in areas with poor drainage [38]. The amount of water that can seep into subsurface formations is determined by the type of soil, which affects the prevalence of flood-prone zones [39]. Soil type directly affects how quickly water drains because of its innate characteristics, which include texture, degree of permeability, and structure [40]. The relationship between soil type and flood susceptible zoning mainly depends on the available soil type in the area. The occurrence of floods is closely linked to soil types, as certain soils, such as clays and silts found in floodplains, can retain water and exacerbate flooding conditions, while sandy soils may allow for better drainage and reduced flood hazard. The soil map for the present study was extracted from the FAO digital soil map of the world. A weight of 0.03 has been assigned to the soil type map.

2.3.4 Elevation

Elevation is a critical factor in flood risk modeling, as it influences the movement of water during flood events; water naturally flows downhill along the path of least resistance, which typically corresponds to the steepest descent [41]. Elevation affects the water discharge rate significantly because water flows from high altitudes to low elevations; hence, flood risks are more common in low-elevation areas than in high-elevation areas [42]. The elevation of the study area is derived from the DEM of the catchment. The relationship between flood occurrence and topographic elevation maps is important and has an inverse relationship with flood zones: high elevated areas have a low probability for flood hazard zones and low land areas have relatively high susceptibility to flood probability zones due to their tendency to collect and retain water, especially during heavy rainfall or when nearby water bodies overflow. A weight of 0.22 has been assigned to the Elevation map.

2.3.5 Slope

The gradient of a slope significantly affects both the volume and direction of surface runoff and subsurface drainage reaching a specific location, as it plays a crucial role in determining how precipitation contributes to streamflow by regulating the duration of overland flow, subsurface flow, and infiltration [43]. Land slope states the amount of inclination of the surface to the horizontal. The slope is a significant factor in identifying flood-prone zones [44]. Similar to elevation, land slope has an inverse relationship with flood probability zones: a highly slopy area has low susceptibility to flood hazard and flat slopes have relatively higher susceptibility to flood. The relationship between flood occurrence and slope maps is crucial, as steeper slopes can lead to increased runoff and faster water flow during heavy rainfall, thereby heightening the hazard of flooding in those areas. The land slope map for the weight overlay analysis was produced on the ArcGIS workspace using the spatial analysis surface tool. A weight of 0.19 has been assigned to the slope theme.

2.3.6 Topographic wetness index (TWI)

The Topographic Wetness Index (TWI) measures the likelihood of water accumulation on slopes by accounting for the effects of gravity on water movement [45]. This has important implications for the occurrence of floods. A steep slope produces deeper water, as shown by a high value on the TWI index, which measures the water's ability to collect [46]. The relationship between flood occurrence and the TWI map is significant, as areas with higher TWI values indicate greater soil moisture and water accumulation potential, making them more susceptible to flooding during heavy rainfall events. TWI was calculated using the following Eq. (1) [47–49].

$$TWI = \ln\left(\frac{As}{\tan \beta}\right) \tag{1}$$

where the slope angle at the site is represented by tan β and the study area is represented by As, respectively. The TWI theme layer has been given a weight of 0.06.

2.3.7 Land use/land cover (LULC)

LULC is the result of land transformation features, while land use refers to human activities on land for a variety of purposes. Based on several studies, the main river basin is dominated by seven different land cover patterns, most of which are crop, range, and water land that significantly affect the possibility of flood hazard zone maps. The relationship between flood occurrence and land use/land cover maps is critical, as changes in land use such as urbanization and the conversion of natural landscapes to impermeable surfaces can significantly increase runoff and reduce infiltration, thereby heightening flood hazard in affected areas. Regions dominated by vegetation, especially forests or trees, which have a high capacity to absorb water into the soil, ultimately have a low susceptibility for flooding [50]. The land use land cover map for the weight analysis was derived from sentinel 2 10 m resolution remote sensing imagery. Esri land cover shows effective and higher efficiency based on different validated study results. A weight of 0.10 has been assigned to the LULC theme.

2.3.8 Distance from river

In determining the food hazard zones and the food hazard index, the distance from the river network component is crucial [51]. Distance from the river is an important factor in determining the flood susceptibility zones. The areas near the river are more vulnerable whether it is a normal flood or flash flood [52]. The closer one is to a river's edge, the more perilous the dance with floodwaters becomes, as nature's relentless embrace knows no boundaries. The distance from the river map is worked on ArcGIS workspace using the Euclidian distance spatial analysis tool. A weight of 0.12 has been assigned to the distance from a river theme.

2.3.9 Normalized difference vegetation index (NDVI)

The most important factor influencing surface runoff in a watershed is the density of vegetation cover in the area [53]. The NDVI measures vegetation density in an area, highlighting that regions with low vegetation density are particularly vulnerable to flooding because they possess significantly reduced soil infiltration capacity [54]. The variation of NDVI scores is -1 to 1. The NDVI can provide a good result for the delineation of vegetation, water bodies, and soil moisture levels [55]. Research has shown that the NDVI is useful for distinguishing between the types of forests that are evergreen and seasonal, as well as for savannah, thick forest, non-forest, and agricultural lands [56]. NDVI has an inverse relationship with floods where higher NDVI values indicate a lower probability of flooding [57]. The NDVI value for the catchment was computed using Eq. (2) adopted from [58]. A weight of 0.04 has been assigned to the NDVI theme.

$$NDVI = \frac{NIR\ band - R\ band}{NIR\ band + R\ band} \tag{2}$$

whereas R stands for the red band and NIR for the near-infrared band. Regarding Landsat 8, NIR is associated with Band 5, and Red is associated with Band 4.

2.3.10 Curvature

The Curvature feature characterizes the slope's curvature and contour, using its second derivative to determine the surface's concavity or convexity [50]. The slope's contours and curvature are represented by the curvature attribute. Curvature significantly influences the flood water budget by delineating runoff patterns; regions with negative curvature indicate areas where water converges, whereas positive curvature represents convex surfaces, zero indicates flat terrain, and negative values signify concave surfaces, effectively distinguishing between divergent and convergent runoff zones [59]. It determines whether the surface is concave or convex based on its second derivative [46]. The most influential factor prone to flooding is flat, followed by concave and convex [60]. Flat areas highly contribute to water accumulation, depending on the surrounding topography and drainage patterns. There is a significant correlation between the development of floods and curvature maps. This is because convex regions promote drainage, which lowers the probability

Table 2 Saaty's Scale [63, 64]

Scale	Definition	Explanation
1	Equal importance	Each of the two actions contributes equally to attaining the outcome
3	Moderate importance	Knowledge and discernment slightly prefer one activity to another
5	Essential or strong importance	One activity is greatly preferred over another by knowledge and expertise
7	Very strong importance	Activity is highly encouraged, and the advantage it offers is proven in real-world situations
9	Extreme importance	The strongest level of confirmation is present in the data that supports one behavior over another
2,4,6,8	Intermediate values between the judgment	Whenever a compromise is required

Table 3 PCA of eleven themes

Fac	El	Sl	Rf	Dfr	LULC	DD	TWI	NDVI	St	Crv
El	*1*	2	2	2	2	4	3	5	6	7
Sl	1/2	*1*	2	2	3	3	4	4	4	7
Rf	1/2	1	*1*	2	2	3	3	4	4	6
Dfr	1/2	1/2	1/2	*1*	2	3	3	3	3	5
LULC	1/2	1/3	1/2	1/2	*1*	2	2	3	4	5
DD	1/4	1/3	1/3	1/3	1/2	*1*	2	2	3	3
TWI	1/3	1/4	1/3	1/3	1/2	1/2	*1*	2	2	3
NDVI	1/5	1/4	1/4	1/3	1/3	1/2	1	*1*	1	2
St	1/6	1/4	1/4	1/3	1/4	1/3	1/2	1	*1*	2
Crv	1/7	1/7	1/6	1/5	1/5	1/3	1/3	1/2	1/2	*1*
Sum	4.09	5.56	7.33	9.03	11.78	17.67	19.33	25.50	28.50	41.00

of flooding, while concave areas tend to collect and retain water, increasing for the occurrence flooding. The curvature map was adjusted and given a weight of 0.02.

2.4 Weighting and ranking using AHP

There is no set list of factors to take into account when utilizing MCDM to determine food sensitivity, and there is no standard method for choosing the factors [61]. Appropriate weight assignment for every theme attribute is necessary as the effects of flood events on different subject levels vary. This method allows us to determine the weights of hierarchically nonstructured or particular hierarchical level criteria concerning those belonging to a higher level [62]. The first step is to create a pairwise comparison matrix (PCM) using Saaty's (1–9) relative importance scale Table 2. The ratings are typically assigned between 1 (equal importance) and 9 (high importance). The importance of these influencing elements is evaluated based on their ability to react to the occurrence of flood occurrences. In addition, the weights were determined by taking into account the evaluation of prior studies, expert suggestions, and practical experience.

A high-weight component represents a theme layer that significantly affects the flood danger zone, while a low-weight parameter represents a layer that has little effect. By assigning a numerical value to each parameter, a paired-wise comparison matrix was constructed to assess each parameter's influence on flood occurrences. The factors that were given the most significance include slope, elevation, rainfall, and distance from the river. Slope and elevation received more weight because of their respective relevance in possible distribution and flood hazard mapping [65, 66], because We have recognized that these factors are essential within the catchment area and play a significant role in determining water flow and accumulation during flood events. Elevation affects the probability of an area experiencing flooding, as lower-lying regions are more vulnerable to being submerged. Meanwhile, slope influences the speed at which water runs off the land; steeper slopes can accelerate water movement, heightening the flood risk for areas downstream. Collectively, these elements offer critical insights into the dynamics of flooding, making them indispensable for precise flood risk evaluations. Intermediate weight has been assigned to LULC, DD, and TWI. The lowest weights have been assigned to NDVI, and curvature (Table 3). Thereafter, pairwise comparison matrices of assigned weights to different thematic layers

Table 4 NPCA of eleven themes

Fac	El	Sl	Rf	Dfr	LULC	DD	TWI	NDVI	St	Crv
El	0.2443	0.3597	0.2727	0.2214	0.1697	0.2264	0.1552	0.1961	0.2105	0.1707
Sl	0.1222	0.1799	0.2727	0.2214	0.2546	0.1698	0.2069	0.1569	0.1404	0.1707
Rf	0.1222	0.0899	0.1364	0.2214	0.1697	0.1698	0.1552	0.1569	0.1404	0.1463
Dfr	0.1222	0.0899	0.0682	0.1107	0.1697	0.1698	0.1552	0.1176	0.1053	0.1220
LULC	0.1222	0.0600	0.0682	0.0554	0.0849	0.1132	0.1034	0.1176	0.1404	0.1220
DD	0.0611	0.0600	0.0455	0.0369	0.0424	0.0566	0.1034	0.0784	0.1053	0.0732
TWI	0.0814	0.0450	0.0455	0.0369	0.0424	0.0283	0.0517	0.0784	0.0702	0.0732
NDVI	0.0489	0.0450	0.0341	0.0369	0.0283	0.0283	0.0259	0.0392	0.0351	0.0488
St	0.0407	0.0450	0.0341	0.0369	0.0212	0.0189	0.0259	0.0392	0.0351	0.0488
Crv	0.0349	0.0257	0.0227	0.0221	0.0170	0.0189	0.0172	0.0196	0.0175	0.0244

Sl-slope, El-elevation, Dfr-distance from river, TWI-topographic wetness index, St-soil type, Rf-rainfall, DD-drainage density, LULC- land use land cover, NDVI-normalized difference vegetation index, and Cvr-curvature

Table 5 Saaty's ratio index for a variety of n

n	1	2	3	4	5	6	7	8	9	10	11
RI	0	0	0.58	0.90	1.12	1.24	1.32	1.41	1.49	1.51	1.51

and their classes are constructed using [67] AHP and weights normalized by the eigenvector approach to reduce the subjectivity involved. To produce the Normalized Pairwise Comparison Matrix (NPCM), all column values were combined and divided by the sum of the columns. The normalized weight of each variable was determined by averaging all values of the appropriate rows in the NPCM Table 4. All the normalized weights added together are equal to one.

The consistency of the judgment matrix should be evaluated with the calculation of the consistency index (CI) which is defined in Eq. (3):

$$CI = \frac{\lambda_{\max} - 1}{n - 1} \tag{3}$$

where CI is the consistency index, n is the number of factors used in the analysis and $\lambda_{\max}$ is the maximum or principal eigenvalue of the judgment matrix and could be calculated using Eq. (4) [68].

$$\lambda_{\max} = \frac{C_1 + C_2 + C_3 + \ldots + C_n}{n} \tag{4}$$

where n is the number of criteria, and C1 to Cn is the λ or eigenvalue value. To calculate the eigenvalue initially, the corresponding variable weight was multiplied by each column of the Pairwise Comparison Matrix. We were then able to determine the weighted sum value by adding up all of the rows. After that, by dividing column elements by the column sum will be obtained. In this research, a λ max value of 11.52 was obtained. Equation (5) is used to calculate the consistency ratio (CR) coefficients.

$$CR = \frac{CI}{RI} \tag{5}$$

where CI is the consistency index. The value of CI was obtained from Saaty's 1–9 scale. RI (random consistency value) of eleven criteria that correspond to a CR value of 1.51 was used as shown in Table 5. To ensure consistency, the pairwise comparison matrix for consistent weights should have a CR value of below 0.1. If not, the associated weightage has to be reexamined to prevent contradiction.

Saaty has opined that a CR of 0.10 or less is acceptable to continue the analysis [67]. If the consistency value is greater than 0.10, the judgment needs to be reviewed to identify the root reasons for the inconsistency and make the necessary corrections. The measure of consistency, called consistency index (CI), is given as 1.51, so the consistency ratio can be calculated as follows:

$$CR = \frac{0.04}{1.51} = 0.026$$

Consequently, a weighted analysis was carried out and the study's consistency ratio was found to be within a reasonable range. All influential parameters' thematic layers were categorized to values between one and five according to how they affected the likelihood of flood events. Those who are highly suitable for flood event occurrence will have a higher value, and those with low suitability will have a much lower value namely: 1 denotes extremely low, 2 low, 3 intermediate, 4 high, and 5 very high.

2.5 Weight overlay analysis

The Flood hazard Zone Index (FRZI) is generated by integrating multiple thematic layers within a GIS environment. This process involves the extraction and combination of various datasets that contribute to the occurrence of floods. This is done by weighted linear combination as described in Eq. (6).

$$FRZI = \sum_{w=1}^{m} \sum_{1}^{n} (W_j \times X_j) \tag{6}$$

Here FRZ is the flood hazard zone index, X_i is the normalized weight of the i^{th} feature of the thematic layer, W_j is the normalized weight of the j^{th} theme, n is the overall number of classes in a theme, and m is the entire number of themes. Finally, the flood hazard zone index map was reclassified into four categories: negligible, low, intermediate, high, and severe flood-prone zones. All assigned weights, ranks, and subclass descriptions are provided in Table 6.

2.6 Result validation

The validation of flood hazard zone simulations is crucial because they provide reliable confirmation in flood mitigation and management techniques. It is essential to verify flood hazard maps using observed flood occurrence points to ensure their credibility. When using prediction models in research, validation is a crucial step. The resulting map of the potential flood hazard zone was validated using observed flood data. The Receiver Operating Characteristic Curve (ROC) and Area Under the Curve (AUC) were used to assess the potential flood hazard zone map's accuracy. One of the most widely used metrics of performance is the ROC) curve, which has been used in many hydrological and geo-environmental studies [69]. The ROC curve plots the false-positive rate on the X-axis and the true-positive rate on the Y-axis [70]. An AUC of 0.5 to 0.6 is often regarded as inadequate, 0.6 to 0.7 as adequate 0.7 to 0.8 as acceptable, 0.8 to 0.9 as excellent, and greater than 0.9 as remarkable Table 6.

3 Results

3.1 Generation of thematic layers

All map layers were generated using the ArcGIS 10.8 working platform. The TWI directly affects flood susceptibility zoning. The results revealed that the values ranged from 2.905 to 24.57. The central part of the catchment is topographically wet and the western part has a relatively low TWI value. The catchment is comprised of three major soil types: eutric cambisol, eutric nitosol, and pellic vertisol. Among them, the pellic vertisol soil type has a high ranking, owing to its substantial response to flood occurrence, followed by eutric nitosol having a rank of 3, and eutric cambisol with a rank of 2. The pellic vertisol soil type occupied more than 50% of the land and was distributed throughout the central, northern, and southern part of the catchment, eutric nitosol was distributed over the northern edge and southern part of the catchment, eutric cambisol was about the western part of the catchment. The distance from the river can greatly affect flood susceptibility zoning and result in higher weights in the present study. The distance from the river map of the catchment is classified into five classes, the distance from 0 to 140 has a higher rank, and a distance of over 3000 has a lower rank for flood susceptibility. The highest distance of 18,298 m from a river was observed in the catchment. NDVI map distribution for the present study was computed using bands 4 and 5 of Landsat 8 data. The NDVI values for the catchment range from − 0.2355 to 0.01212. As NDVI has an inverse relationship with flood occurrence, areas with high

Table 6 Weight and ranking of factors

Factors	Low range	Value	Flood probability	AHP weight	Percent (%)
Elevation	1764–1895	5	Very high	0.22	22
	1896–2060	4	High		
	2061–2255	3	Intermediate		
	2256–2390	2	Low		
	2391–3091	1	Very low		
Slope	0–4	5	Very high	0.19	19
	4–10	4	High		
	10–21	3	Intermediate		
	21–30	2	Low		
	> 30	1	Very low		
Rainfall	428–480	1	Very low	0.15	15
	481–511	2	Low		
	512–546	3	Intermediate		
	547–579	4	High		
	580–613	5	Very high		
Soil type	Eutric cambisol	2	Low	0.03	3
	Eutric nitosol	3	Intermediate		
	Pellic vertisol	5	Very high		
Drainage Density	0.272–1.79	1	Very low	0.07	7
	1.79–2.43	2	Low		
	2.43–2.98	3	Intermediate		
	2.98–3.34	4	High		
	3.34–4.15	5	Very high		
TW1	2.905–6.814	1	Very low	0.06	6
	6.815–8.683	2	Low		
	8.684–11.15	3	Intermediate		
	11.16–14.72	4	High		
	14.73–24.57	5	Very high		
Curvature	Convex	3	Intermediate	0.02	2%
	Flat	5	Very high		
	Concave	1	Very low		
Distance from river	< 140	5	Very high	0.12	12
	140–150	4	High		
	500–1500	3	Intermediate		
	1500–3000	2	Low		
	> 3000	1	Very low		
LULC	Barren land	4	High	0.10	10
	Forest land	1	Very low		
	Urban area	5	Very high		
	Waterbody	5	Very high		
	Crops land	3	Intermediate		
	Flooded vegetation	5	Very high		
	Grassland	2	Low		
NDVI	< 0.012	5	Very high	0.04	4
	0.012–0.12	4	High		
	0.12–0.173	3	Intermediate		
	0.173–0.256	2	Low		
	0.256–0.584	1	Very low		

NDVI values, such as western forest lands of the catchment, have low susceptibility to flooding, and the wetter waterbodies of the catchment with low NDVI values were more prone to flooding. The topographic elevation of the catchment had a relatively higher weight owing to its relative importance. The elevation of the catchment varied between 1764 and 3091 m and was classified into five distinct-ranked zones. The highly elevated upstream area of the catchment has a low rank, whereas the low elevated parts of the downstream catchment are highly ranked. The spatial distribution of the thematic layers is shown in Fig. 3a and b.

Rainfall is known to have a major effect on flooding. The IDW manipulation in the ArcGIS workspace revealed that northwestern parts of the catchment receive a higher amount of rainfall. The study area's highest rainfall is 613 mm, and its lowest rainfall is 428 mm. Drainage density is directly related to the flood probability zones. The drainage density of the catchment varied between 0.2722 and 4.1546. The final generated layer was classified into five respective classes, and a higher drainage density area was considered a flood-prone area with a high rank. The slope in the present study was the one that received a higher weight owing to its higher relative importance. The slope of the catchment was expressed as a percentage and ranged from 0 to 200.48%. Slopes with higher values had smaller ranks and those with low values received higher ranks. The land cover theme was another important factor included in this study. According to the Esri Sentinel 2 land cover map, the catchment has seven distinct land cover classes: built-up areas, water bodies, barren land, agricultural land, flooded vegetation, forest land, and range land. Areas such as water bodies, urban areas, and flooded vegetation have increased due to their sensitivity to flood occurrence, and areas such as forest and grassland had a low rank, and cropland had a medium rank. The low-ranked thematic layer was curvature. Curvatures in the Modjo catchment are classified into three classes: convex, concave, and flat. The classification is based on the curvature section of the spatial analysis tool. Values are categorized as concave as long as they range above 0.45, as flat when they range between 0.45 and − 0.45, and convex when they range below − 0.45. In the current study, the flood vulnerability of flat regions was ranked as medium, convex low, and concave high. A similar arrangement was also made by [6].

3.2 Flood hazard zone identification

Upon combining all of the normalized thematic layers in a GIS environment and converting them into a raster format, the study area's flood hazard zone map was created. Substantial portions of the catchment area have been effectively identified by the mapping process employing MCDM approaches as having a high and sever potential for flood hazard. This in-depth research draws attention to particular places that have a higher probability of flooding, highlighting the significance of these areas in flood hazard assessments. The identification of such significant zones is critical for understanding the potential impacts of flooding and for informing future management and mitigation strategies aimed at reducing flood-related hazards. Five subclasses were created from the catchment's possible flood hazard zones, namely: severe, high, intermediate, low, and negligible. This study reveals that about 0.2% (244.7343 ha), 28.754% (34,322.6544 ha), and 56.03% (64,309.5245 ha) of the Modjo catchment represent negligible, low, and intermediate flood hazard zone categories, while values 17.164% (20,489.1534 ha), and 17.164% (20,489.1534 ha) were considered as high potential for flood hazard zone. The spatial distribution of the potential zones is shown in the above Fig. 4.

The flood hazard map gives important information about where areas that are likely to flood are located in the catchment region. It shows that most of these areas are in the lower parts of the catchment. Classifying sub watersheds is crucial for effective watershed management, particularly in identifying and prioritizing areas that are more prone to flooding. By breaking down larger watersheds into smaller sub watersheds, it becomes easier to analyze specific characteristics and vulnerabilities of each area. The sub-watersheds in the upper part and the northern central part of the catchment, which is more mountainous, have much less susceptibility to flooding. The mountainous regions act as natural barriers that can absorb and redirect water flow, thereby mitigating flood risks. In areas where the terrain is less rugged, such as the lower elevations, water can accumulate more easily, leading to a higher likelihood of flooding during heavy rainfall events. This big difference shows how the land and the shape of the region affect flood hazard. In particular, the lower parts, especially those near the River Modjo, have a higher probability of flooding, while the higher elevations and rough terrain in the upper areas act as natural barriers that help reduce the effects of flooding. Sub-classes areal variation is shown in Table 7.

The classification of flood hazard zones into negligible, low, intermediate, high, and severe categories has significant implications for local communities. With 74.12% of the area falling into the intermediate zone, communities face a moderate risk of flooding, which necessitates proactive measures for disaster preparedness and response. This substantial proportion indicates that many residents may not perceive an immediate threat, potentially leading to complacency regarding flood risk management. The presence of high (8.44%) and severe (0.0012%) zones highlights areas that require

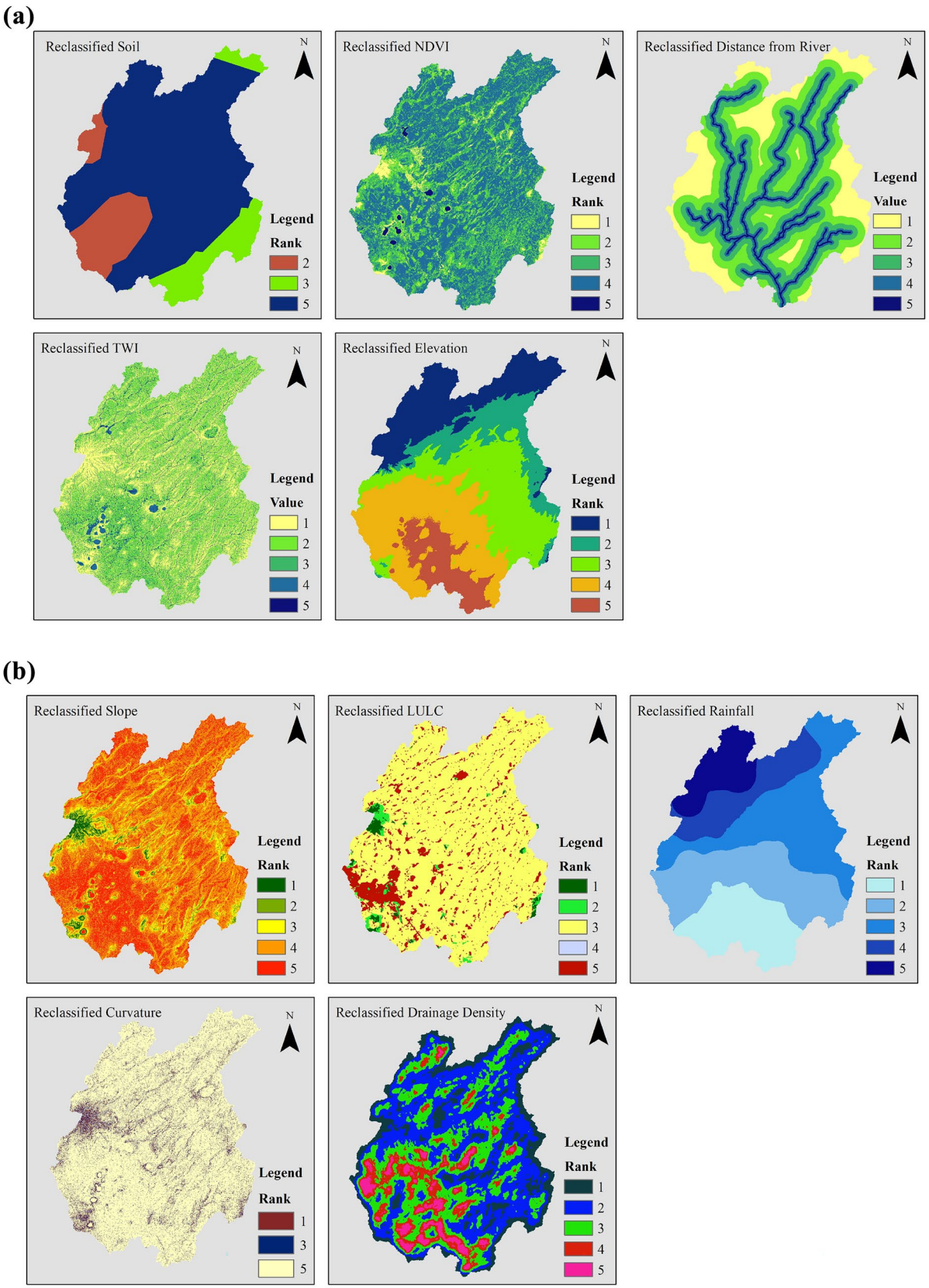

Fig. 3 **(a)** Thematic layers for overlay analysis. **(b)** Thematic layers for overlay analysis

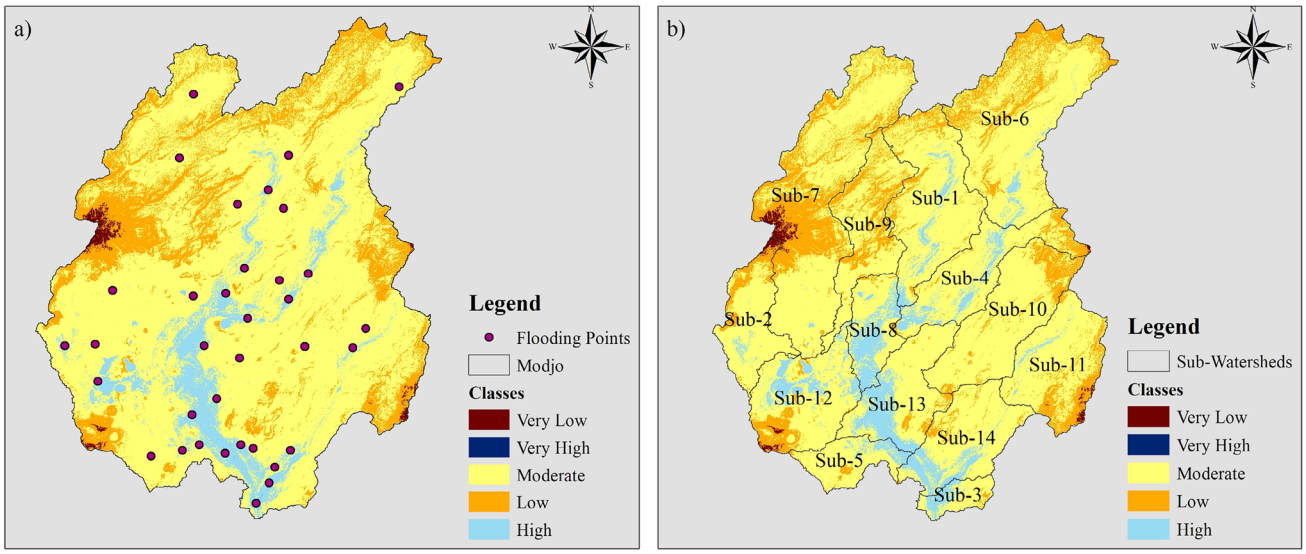

Fig. 4 Potential zones for flood hazard (**a**) flood inventory points (**b**) sub watersheds

Table 7 Numerical description for flood hazard zones

Value	Count	Area (hectares)	Area (Km^2)	Percentage (%)	Flood map zone
1	10828	974.52	9.7452	0.686497	Negligible
2	263961	23756.49	237.5649	16.73516	Low
3	1169199	105227.9	1052.279	74.12736	Intermediate
4	133276	11994.84	119.9484	8.449715	High
5	20	1.8	0.018	0.001268	Sever
Total	1577284	141955.6	1419.556	100	

urgent attention and targeted interventions, such as enhanced infrastructure, flood defenses, and community awareness programs. Local governments may need to prioritize these zones for funding and resources to mitigate potential flood impacts effectively. Moreover, the negligible (0.686%) and low (16.73516%) zones suggest that while these areas are less at risk, they should not be overlooked in planning efforts.

3.3 Validation of the results

Ensuring the accuracy of flood hazard mapping data is crucial since it facilitates policy formulation. It encourages integrated management techniques, enhances engagement with stakeholders, and makes the most use of available resources. When combined, these factors result in flood hazard management strategies that are more efficient and greatly increase community resilience to flooding incidents. Typically, in the context of flood hazard zone map validation, the criterion in the evaluation must reflect the reality of the field, the criterion independence principles, and the conformity of the criterion. The results have been validated with the help of observed flood occurrence data distributed in the study area. Validation consisted of five classes equal to the stone flood hazard potential zones: strongly agree, agree, slightly disagree, agree, and strongly disagree. Out of the twenty-nine data points, twenty-three were in agreement and six provided some disagreement with the recorded potential zones. There was no observed flooding in the low and negligible-hazard zones as per the validation. In summary, the validated results demonstrate that the forecasts concord well with observed flood evidence (Table 8).

The flood hazard map's prediction accuracy was verified using the Receiver Operating Characteristic (ROC) curve and AUC measurements (Fig. 5). The genuine positive value and the study's ultimate anticipated result are taken into account to create this curve. An accuracy of 0.868 in the prediction was indicated by the results. AUC values greater than 0.8 are generally regarded as excellent and, as a result, acceptable models. The study used a systematic validation approach and obtained

Table 8 Validation of results using observed flood event data

Id	GCS WGS UTM ZONE 37		Predicted	Remark
	X-coordinate	Y-coordinate		
Modjo01	515837.639	990960.062	High	Agree
Modjo02	515333.607	985348.238	High	Agree
Modjo03	505808.588	997386.804	Intermediate	Slightly disagree
Modjo04	497275.758	976683.116	Intermediate	Slightly disagree
Modjo05	527551.869	998156.081	High	Agree
Modjo06	510658.807	969524.491	Intermediate	Slightly disagree
Modjo07	509150.679	959461.485	High	Agree
Modjo08	504652.753	959778.986	High	Agree
Modjo09	516051.357	959752.527	High	Agree
Modjo10	510,809.289	960347.841	High	Agree
Modjo11	508262.669	965209.570	High	Agree
Modjo12	514381.171	957999.659	High	Agree
Modjo13	512139.484	959985.097	High	Agree
Modjo14	512412.535	954117.261	Sever	Very agree
Modjo15	513801.600	956339.766	High	Agree
Modjo16	495704.064	967055.412	High	Agree
Modjo17	495426.251	970984.483	High	Agree
Modjo18	514865.227	977699.621	Intermediate	Slightly disagree
Modjo19	522660.529	970615.388	High	Agree
Modjo20	523995.523	972610.100	High	Agree
Modjo21	517550.424	970757.880	High	Agree
Modjo22	515857.088	975732.057	High	Agree
Modjo23	517920.842	978430.812	Intermediate	Slightly disagree
Modjo24	506931.792	970814.325	High	Agree
Modjo25	506442.312	960350.033	High	Agree
Modjo26	505648.560	963525.039	High	Agree
Modjo27	501352.107	959157.277	High	Agree
Modjo28	510470.040	985752.717	Intermediate	Slightly disagree
Modjo29	504318.465	990647.519	High	Agree

satisfactory validation results; nevertheless, for more accurate and trustworthy verified conclusions, more flood inventory data need to have been incorporated.

3.4 Limitations

The pursuit of reliable and impactful research necessitates a transparent acknowledgment of inherent limitations. This study, while offering valuable insights, is subject to constraints that should be carefully considered to inform future investigations. One key limitation stems from the restricted availability of observed flood inventory data. This scarcity of reliable, observed data directly hampered the comprehensive validation and rigorous examination of the developed technique. A more robust model requires a considerably larger and more diverse dataset representing a wider range of flood events and magnitudes, allowing for a more thorough assessment of model accuracy and predictive capability. The availability of such data would enable researchers to assess the model's performance under various hydrological conditions, increasing confidence in its applicability and predictive power.

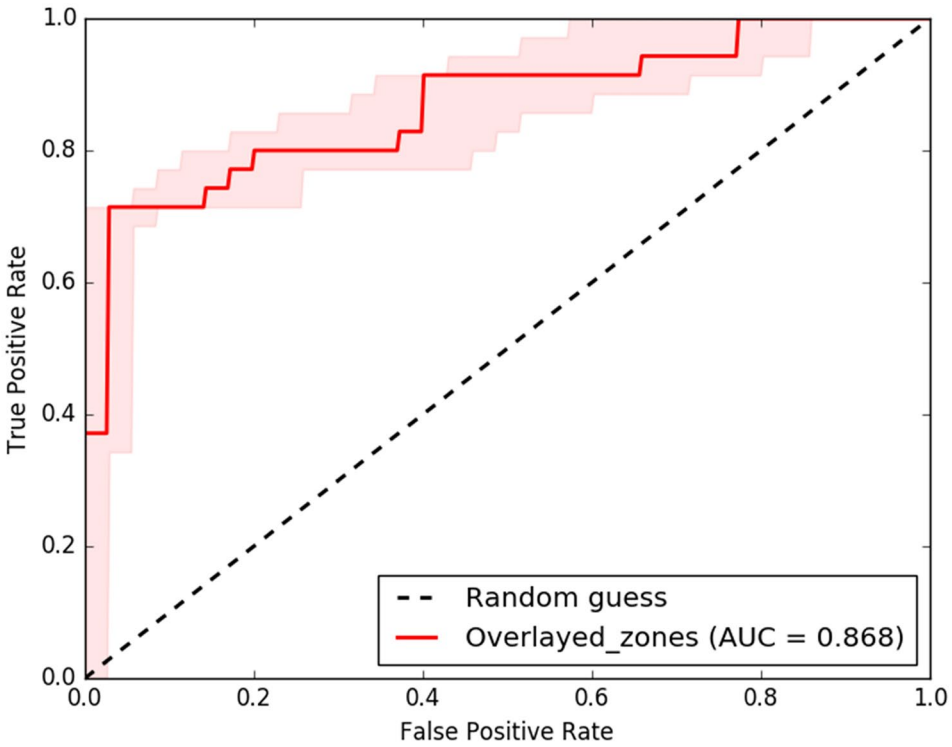

Fig. 5 ROC curve for result validation

4 Discussions

The impact of weighting and ranking was visible in the final generated potential flood hazard zones. The thematic layers that carry higher weights, such as Slope, elevation, rainfall, and distance from the river, closely align in spatial distribution with the final produced spatial distribution map. Areas of low elevation and slope, particularly in the central mountainous regions, have been classified as low potential zones. In contrast, lowlands and flatter regions, which are ranked highly, show greater potential for Flood hazard zones. The thematic layers assigned intermediate weights, LULC, DD, and TWI, have a substantial but less pronounced effect on the potential zone map. Conversely, thematic layers with lower weights have minimal impact and visibility on the final potential zone map. In this context, it was revealed that weight assignment is a crucial and fundamental aspect of the AHP process.

Flood mapping using MCDM faces significant challenges that prevent it from achieving 100% efficiency and validation. One major limitation is the subjectivity in criteria weighting, as different stakeholders may prioritize factors like hydrology, land use, and socio-economic considerations differently, leading to inconsistent results. Additionally, the quality and availability of data can significantly affect the accuracy of the flood maps; often, data may be incomplete or outdated, introducing uncertainty into the models. MCDM also struggles with capturing the complex interactions among various criteria influencing flood hazardss, which may result in oversimplification. Moreover, environmental conditions are constantly changing due to climate change and urban development, which may render existing models less applicable over time. Lastly, the difficulty in validating these models against rare observed flood events adds another layer of uncertainty, making it challenging to ensure complete accuracy in flood hazard assessments.

The outcomes of the present investigation show a considerable degree of consistency with findings from prior studies carried out using similar geographic and environmental conditions, which utilized MCDM and geospatial techniques to delineate flood hazard areas. Research works by [5, 16, 46, 61, 71] conducted MCDM flood hazard mapping, placing considerable emphasis on slope and elevation weighting, and identified a significant flood hazard zone within their study area. By affirming the trends and observations identified in previous studies, this research offers additional validation and deepens our understanding of the topic. The similarities in outcomes imply that the factors influencing flood event conditions have a stable impact, which is vital for future research and applications in this area.

These results have important environmental implications, as they highlight the urgent need for effective flood management strategies to protect ecosystems and biodiversity. Additionally, the social implications are profound;

communities in flood-prone areas may face increased vulnerability, necessitating policies that promote resilience and support for affected populations. Furthermore, the findings can inform policymakers about the necessity of integrating flood risk assessments into urban planning and development policies, ensuring sustainable growth while mitigating potential disaster impacts. Overall, this research underscores the interconnectedness of environmental risks and social equity, emphasizing the need for comprehensive strategies that address both ecological and community needs.

As noted above, the presence of flood hazard zones in the Modjo catchment area creates significant potential implications for sustainable development as well as disaster management in the region. It is, therefore, important to highlight these zones, to improve flood management systems and strategies including the provision of proper drainage systems and land-use planning that incorporates flood hazard. Such areas are often prone to hazards that increase the likelihood of suffering economic losses, social dislocations as well as out-migrations, which invariably worsen this setback. In addition, it is pointed out in the study that in-depth education of the residents on the threats and measures to help combat them is very critical in the area to help build resilience and reduce the effects of flooding on the people and the infrastructure within the Modjo catchment area.

5 Conclusions

The objective of this study is to identify and develop potential flood hazard zones employing integrated use of geoinformatics tools through MCDM over Modjo catchment, central Ethiopia. Flood hazard susceptible zones are created using a variety of multiple-influencing factors including curvature, NDVI, drainage density, curvature, rainfall, soil type, elevation, slope, topographic wetness index, and land use/land cover for the hazard zone. These influencing factors' features were given appropriate weightage based on their reaction to flood occurrence, local conditions, and experts' suggestions. Weight overlay analysis produced 22% for elevation, 19% for slope, 15% for rainfall, 12% for distance from the river, 10% for land use land cover, 7% for drainage density, 6% for TWI, 4% for NDVI, 3% for soil type, and 2% for curvature. The flood hazard zones were obtained by overlaying all the thematic maps by weighted overlay methods using the spatial analysis tool in ArcGIS 10.8. The catchment flood hazard zone was generated and categorized into four groups: negligible, low, intermediate, high, and severe. The negligible, low, intermediate, high, and severe susceptible zones were represented by 0.686% (9.74 km^2), 16.73% (237.56 km^2),74.12% (1052.28 km^2), 8.44% (119.94 km^2), and 0.0012% (0.018 km^2), respectively. The weighting and ranking process was effectively represented in the final flood hazard zone map. The results indicate that a significant portion of the catchment area is at hazard. Ultimately, 29 observed flood datasets were utilized to validate the findings, achieving an accuracy of over 85% and an area under the ROC curve of 0.868. Most of the flood point data was concentrated in the high and severe regions. This study significantly enhances the understanding of potential flood sites within the catchment, providing a foundational framework for future initiatives. The findings are expected to positively influence current management strategies, enabling them to sustainably address the flood susceptibility issue faced by the local community. The study suggests that future research should explore alternative methodologies, including Hydrological and Hydraulic Modeling, Statistical Methods, and Machine Learning and Data Mining. It is recommended to compare the results from these approaches with those obtained from Multi-Criteria Decision-Making (MCDM) methods to enhance the understanding of flood risk assessment and improve predictive accuracy. The study highly recommends finding out more flood inventory data to explore the change in the validation results. Incorporating additional influencing factors such as aspect, lithology, stream flow index, geomorphology, modified normalized water index, and groundwater table into the AHP analysis could enhance our understanding of whether conditions improve. It is also advised that relevant authorities assess or use the present study flood hazard zone results in the Modjo catchment to identify effective strategies to harness flood hazard challenges. This can be achieved by engaging local communities in data collection to improve accuracy and creating interactive web platforms for real-time flood risk information. Establishing protocols for continuous data evaluation, fostering collaboration among government agencies and NGOs, focusing on precise floodplain management, and using mapping results to guide targeted flood control infrastructure in high-risk areas will further enhance flood hazard mapping and mitigation efforts.

Author contribution B. B. and W. T. conceptualized the study and proposed methodology, B. B. write and edit the manuscript; W. T. supervised the study, reviewed the manuscript, validated the results, and updated the manuscript. All authors commented on previous versions of the manuscript. All authors approved the final submitted version of the manuscript.

Funding This research received no external funding.

Availability of data and materials The data that support the findings of this study are available from the corresponding author, upon reasonable request.

Declarations

Competing interests The authors declare no competing interests.

References

1. Safaripour M, Monavari M, Zare M. Flood risk assessment using GIS (case study: Golestan province, Iran). Pol J Environ Stud. 2012;21(6):1817–24.
2. Ward PJ, et al. Review article: natural hazard risk assessments at the global scale. Nat Hazard Earth Syst Sci. 2020;20(4):1069–96. https://doi.org/10.5194/nhess-20-1069-2020.
3. Jones RL, Guha-Sapir D, Tubeuf S. Human and economic impacts of natural disasters: can we trust the global data? Sci Data. 2022;9(1):1–7. https://doi.org/10.1038/s41597-022-01667-x.
4. Reguero BG, Renaud F, Di Sabatino S, Jongman B, Van Zanten B, Beck MW. Nature-based solutions for natural hazards and climate change. Front Environ Sci. 2023. https://doi.org/10.3389/978-2-83251-158-9.
5. Mokhtari E, Mezali F, Abdelkebir B, Engel B. Flood risk assessment using analytical hierarchy process: a case study from the Cheliff-Ghrib watershed, Algeria. J Water Clim Chang. 2023;14(3):694–711. https://doi.org/10.2166/wcc.2023.316.
6. AlAli AM, Salih A, Hassaballa A. Geospatial-based analytical hierarchy process (AHP) and weighted product model (WPM) techniques for mapping and assessing flood susceptibility in the Wadi Hanifah drainage basin, Riyadh region, Saudi Arabia. Water (Switzerland). 2023. https://doi.org/10.3390/w15101943.
7. Sardhara VK, Charmi P, Patel KC, Patel RJ. Flood risk assessment and utilization of AHP in flood mapping: a comprehensive review. Int Res J Mod Eng Technol Sci. 2024;12:1893–902. https://doi.org/10.56726/irjmets18081.
8. Swain KC, Singha C, Nayak L. Flood susceptibility mapping through the GIS-AHP technique using the cloud. ISPRS Int J Geo Inf. 2020. https://doi.org/10.3390/ijgi9120720.
9. Gashaw W, Legesse D. Nile river basin. Nile River Basin. 2011. https://doi.org/10.1007/978-94-007-0689-7.
10. AL-Hussein AAM, Hamed Y, Bouri S, Hajji S, Aljuaid AM, Hachicha W. The socio-economic effects of floods and ways to prevent them: a case study of the Khazir river basin northern Iraq. Water (Switzerland). 2023. https://doi.org/10.3390/w15244271.
11. Abegaz R, Xu J, Wang F, Huang J. Impact of flooding events on buried infrastructures: a review. Front Built Environ. 2024;10(April):1–8. https://doi.org/10.3389/fbuil.2024.1357741.
12. Armah FA, Yawson DO, Yengoh GT, Odoi JO, Afrifa EKA. Impact of floods on livelihoods and vulnerability of natural resource dependent communities in Northern Ghana. Water (Switzerland). 2010;2(2):120–39. https://doi.org/10.3390/w2020120.
13. Zhang Y, Li Z, Ge W, Chen X, Xu H, Guan H. Evaluation of the impact of extreme floods on the biodiversity of terrestrial animals. Sci Total Environ. 2021;790(100): 148227. https://doi.org/10.1016/j.scitotenv.2021.148227.
14. Barker P. Mental health ethics: the human context. Ment Heal Ethics Hum Context. 2010;321(November):1–378. https://doi.org/10.4324/9780203839058.
15. Jonkman SN, Curran A, Bouwer LM. Floods have become less deadly: an analysis of global flood fatalities 1975–2022. Nat Hazards. 2024;120(7):6327–42. https://doi.org/10.1007/s11069-024-06444-0.
16. Dano UL. An AHP-based assessment of flood triggering factors to enhance resiliency in Dammam, Saudi Arabia. GeoJournal. 2022;87(3):1945–60. https://doi.org/10.1007/s10708-020-10363-5.
17. Tramblay Y, Villarini G, Zhang W. Observed changes in flood hazard in Africa. Environ Res Lett. 2020. https://doi.org/10.1088/1748-9326/abb90b.
18. Mekonnen TM, Mitiku AB, Woldemichael AT. Flood hazard zoning of upper Awash river basin, Ethiopia, using the analytical hierarchy process (AHP) as compared to sensitivity analysis. Sci World J. 2023. https://doi.org/10.1155/2023/1675634.
19. Mamo S, Berhanu B, Melesse AM. Historical flood events and hydrological extremes in Ethiopia. Extrem Hydrol Clim Var Monit Model Adapt Mitig. 2019. https://doi.org/10.1016/B978-0-12-815998-9.00029-4.
20. Taye MT, Haile AT, Dessalegn M. Flood adaptation and mitigation in the Awash Basin: responding to new climate patterns. Oxford: University of Oxford; 2024. p. 1–44.
21. Hagos YG, Andualem TG, Yibeltal M, Mengie MA. Flood hazard assessment and mapping using GIS integrated with multi-criteria decision analysis in upper Awash river basin, Ethiopia. Appl Water Sci. 2022;12(7):1–18. https://doi.org/10.1007/s13201-022-01674-8.

22. Besha KZ, Demissie TA, Feyessa FF. Comparative analysis of long-term precipitation trends and its implication in the Modjo catchment, central Ethiopia. J Water Clim Chang. 2022;13(11):3883–905. https://doi.org/10.2166/wcc.2022.234.
23. Al Kuisi M, Al Azzam N, Hyarat T, Farhan I. Flood hazard and risk assessment of flash floods for petra catchment area using hydrological and analytical hierarchy (AHP) modeling. Water (Switzerland). 2024. https://doi.org/10.3390/w16162283.
24. Kaya CM, Derin L. Parameters and methods used in flood susceptibility mapping: a review. J Water Clim Chang. 2023;14(6):1935–60. https://doi.org/10.2166/wcc.2023.035.
25. El-Rayes AE, Arnous MO, Helmy AM. GIS-based flash flooding susceptibility analysis and water management in arid mountain ranges: Safaga region, Red sea mountains, Egypt. J Mt Sci. 2023;20(12):3665–86. https://doi.org/10.1007/s11629-023-8142-2.
26. Mourato S, Fernandez P, Pereira LG, Moreira M. Assessing vulnerability in flood prone areas using analytic hierarchy process—group decision making and geographic information system: a case study in Portugal. Appl Sci. 2023. https://doi.org/10.3390/app13084915.
27. Gigović L, Pamučar D, Bajić Z, Drobnjak S. Application of GIS-interval rough AHP methodology for flood hazard mapping in Urban areas. Water (Switzerland). 2017;9(6):1–26. https://doi.org/10.3390/w9060360.
28. Tafese E. Groundwater potential zone mapping using Arc GIS and analytical hierarchy process (AHP) for the case of lower Omo-Gibe Watershed, Omo-Gibe basin, Ethiopia. Glob Challenges. 2022;6(1):2100068.
29. Jhariya DC, Mondal KC, Kumar T, Indhulekha K, Khan R, Singh VK. "Assessment of groundwater potential zone using GIS-based multi-influencing factor (MIF), multi-criteria decision analysis (MCDA) and electrical resistivity survey techniques in Raipur city, Chhattisgarh, India. Aqua Water Inf Ecosyst Soc. 2021;70(3):375–400. https://doi.org/10.2166/aqua.2021.129.
30. Kameswara ASP, Suharjito. Analysis of flood disaster risk factors with geographic information system (GIS) and analytical hierarchy process (AHP) methods in Bekasi city. Int J Eng Trend Technol. 2023;71(4):371–86. https://doi.org/10.14445/22315381/IJETT-V71I4P233.
31. Mallick J, et al. Modeling groundwater potential zone in a semi-arid region of Aseer using Fuzzy-AHP and geoinformation techniques. Water. 2019;11(12):2656. https://doi.org/10.3390/w11122656.
32. Alemu MG, Wubneh MA, Worku TA. Impact of climate change on hydrological response of Mojo river catchment, Awash river basin, Ethiopia. Geocarto Int. 2022. https://doi.org/10.1080/10106049.2022.2152497.
33. Ngwijabagabo H, et al. Groundwater Potential Mapping using Geospatial and AHP Techniques in Eastern Province of Rwanda. Rwanda J Eng Sci Technol Environ. 2023. https://doi.org/10.4314/rjeste.v5i1.4.
34. Pallard B, Castellarin A, Montanari A. A look at the links between drainage density and flood statistics. Hydrol Earth Syst Sci. 2009;13(7):1019–29. https://doi.org/10.5194/hess-13-1019-2009.
35. Akbari M, et al. Identification of the groundwater potential recharge zones using MCDM models: full consistency method (FUCOM), best worst method (BWM) and analytic hierarchy process (AHP). Water Resour Manag. 2021;35(14):4727–45. https://doi.org/10.1007/s11269-021-02924-1.
36. Kerdous ST, et al. A multidisciplinary approach for groundwater potential. Water. 2022;14:1–26.
37. Murasingh S, Jha R Conference paper : identification of groundwater potential zones using remote sensing and GIS in a mine area of Odisha identification of groundwater potential zones using remote sensing and GIS in a mine area of Odisha. 2013. https://doi.org/10.13140/RG.2.1.3374.6644.
38. Basri H, Syakur S, Azmeri A, Fatimah E. Floods and their problems: land uses and soil types perspectives. IOP Conf Ser Earth Environ Sci. 2022. https://doi.org/10.1088/1755-1315/951/1/012111.
39. Morgan H, Hussien HM, Madani A, Nassar T. Delineating groundwater potential zones in hyper-arid regions using the applications of remote sensing and GIS modeling in the eastern desert, Egypt. Sustain. 2022. https://doi.org/10.3390/su142416942.
40. Tehrany MS, Jones S, Shabani F. Identifying the essential flood conditioning factors for flood prone area mapping using machine learning techniques. CATENA. 2019. https://doi.org/10.1016/j.catena.2018.12.011.
41. Al-Kindi KM, Alabri Z. Investigating the role of the key conditioning factors in flood susceptibility mapping through machine learning approaches. Earth Syst Environ. 2024;8(1):63–81. https://doi.org/10.1007/s41748-023-00369-7.
42. Alimi SA, et al. GIS-assisted flood-risk potential mapping of Ilorin and its environs, Kwara state, Nigeria. Remote Sens Earth Syst Sci. 2023;6(3–4):239–53. https://doi.org/10.1007/s41976-023-00093-w.
43. Tariq A, et al. Flash flood susceptibility assessment and zonation by integrating analytic hierarchy process and frequency ratio model with diverse spatial data. Water (Switzerland). 2022. https://doi.org/10.3390/w14193069.
44. Sugianto S, Deli A, Miswar E, Rusdi M, Irham M. The effect of land use and land cover changes on flood occurrence in Teunom Watershed, Aceh Jaya. Land. 2022. https://doi.org/10.3390/land11081271.
45. Fitra J, Debataraja SMT, Lismawaty. Identification of flood vulnerability using the topographic wetness index method in Pantai Labu Baru village Deli Serdang North Sumatera. E3S Web Conf. 2024. https://doi.org/10.1051/e3sconf/202448301014.
46. Waseem M, Ahmad S, Ahmad I, Wahab H, Leta MK. Urban flood risk assessment using AHP and geospatial techniques in swat Pakistan. SN Appl Sci. 2023. https://doi.org/10.1007/s42452-023-05445-1.
47. Arulbalaji P, Padmalal D, Sreelash K. GIS and AHP techniques based delineation of groundwater potential zones: a case study from Southern Western Ghats, India. Sci Rep. 2019;9(1):1–17. https://doi.org/10.1038/s41598-019-38567-x.
48. Owolabi ST, Madi K, Kalumba AM, Orimoloye IR. A groundwater potential zone mapping approach for semi-arid environments using remote sensing (RS), geographic information system (GIS), and analytical hierarchical process (AHP) techniques: a case study of Buffalo catchment, Eastern Cape, South Africa. Arab J Geosci. 2020. https://doi.org/10.1007/s12517-020-06166-0.
49. Khan ZA, Jhamnani B. Identification of groundwater potential zones of Idukki district using remote sensing and GIS-based machine-learning approach. Water Suppl. 2023;23(6):2426–46. https://doi.org/10.2166/ws.2023.134.
50. Mukhtar MA, et al. Integrated flood risk assessment in Hunza-Nagar, Pakistan: unifying big climate data analytics and multi-criteria decision-making with GIS. Front Environ Sci. 2024;12(February):1–18. https://doi.org/10.3389/fenvs.2024.1337081.
51. Osman SA, Das J. GIS-based flood risk assessment using multi-criteria decision analysis of Shebelle river basin in southern Somalia. SN Appl Sci. 2023. https://doi.org/10.1007/s42452-023-05360-5.
52. Majeed M, et al. Prediction of flash flood susceptibility using integrating analytic hierarchy process (AHP) and frequency ratio (FR) algorithms. Front Environ Sci. 2023;10(January):1–14. https://doi.org/10.3389/fenvs.2022.1037547.

53. Koralay N, Kara Ö. Assessment of flood risk in Söğütlü stream watershed of Trabzon province in Turkey using geographic information systems and analytic hierarchy process approach. Nat Hazards. 2024;120(11):9977–10000. https://doi.org/10.1007/s11069-024-06594-1.
54. Vu VT, et al. Predicting land use effects on flood susceptibility using machine learning and remote sensing in coastal Vietnam. Water Pract Technol. 2023;18(6):1543–55. https://doi.org/10.2166/wpt.2023.088.
55. Mukherjee R, Deb P. Application of GIS-based analytical hierarchy process for assessment and mapping of flood risk zone in the lower Ramganga River Basin, Western Gangetic Plain, India. Environ Dev Sustain. 2024. https://doi.org/10.1007/s10668-023-02957-z.
56. Huang S, Tang L, Hupy JP, Wang Y, Shao G. A commentary review on the use of normalized difference vegetation index (NDVI) in the era of popular remote sensing. J For Res. 2021;32(1):1–6. https://doi.org/10.1007/s11676-020-01155-1.
57. Ganjirad M, Delavar MR. Flood risk mapping using random forest and support vector machine. 2023. ISPRS Ann Photogramm Remote Sens Spat Inf Sci. https://doi.org/10.5194/isprs-annals-X-4-W1-2022-201-2023.
58. Das N, Mondal P, Sutradhar S, Ghosh R. Assessment of variation of land use/land cover and its impact on land surface temperature of Asansol subdivision. Egypt J Remote Sens Sp Sci. 2021;24(1):131–49. https://doi.org/10.1016/j.ejrs.2020.05.001.
59. Edamo ML, Bushira K, Ukumo TY. Flood susceptibility mapping in the Bilate catchment, Ethiopia. H2Open J. 2022. https://doi.org/10.2166/h2oj.2022.128.
60. Mujib MA, et al. Assessment of flood hazard mapping based on analytical. Geosfera Indones. 2021;6(3):353–76.
61. Negese A, Worku D, Shitaye A, Getnet H. Potential flood-prone area identification and mapping using GIS-based multi-criteria decision-making and analytical hierarchy process in Dega Damot district, northwestern Ethiopia. Appl Water Sci. 2022;12(12):1–21. https://doi.org/10.1007/s13201-022-01772-7.
62. Legesse A, Abrar H, Esayas Dube E, Likisa Beyene D. AHP based analysis of groundwater potential in the western escarpment of the Ethiopian rift valley. Geol Ecol Landsc. 2021. https://doi.org/10.1080/24749508.2021.1952761.
63. Saaty TL. The analytic hierarchy process-what it is and how it is used. Math Model. 1987;9(3–5):161–76. https://doi.org/10.1016/0270-0255(87)90473-8.
64. Saaty TL. Decision making for leaders: the analytic hierarchy process for decisions in a complex world. Buckinghamshire: RWS publications; 2001.
65. Berhanu KG, Hatiye SD. Identification of groundwater potential zones using proxy data: case study of Megech Watershed, Ethiopia. J Hydrol Reg Stud. 2020. https://doi.org/10.1016/j.ejrh.2020.100676.
66. Arunbose S, Srinivas Y, Rajkumar S, Nair NC, Kaliraj S. Remote sensing, GIS and AHP techniques based investigation of groundwater potential zones in the Karumeniyar river basin, Tamil Nadu, southern India. Groundw Sustain Dev. 2021;14: 100586.
67. Saaty TL. Decision making with the analytic hierarchy process. Int J Serv Sci. 2008;1(1):83–98.
68. Zghibi A, et al. Using analytical hierarchy process and and multi-influencing factors to map groundwater recharge zones in a semi-arid Mediterranean. Water. 2020;12(9):2525.
69. Moghaddam DD, Rahmati O, Haghizadeh A, Kalantari Z. A modeling comparison of groundwater potential mapping in a mountain bedrock aquifer: QUEST, GARP, and RF models. Water (Switzerland). 2020. https://doi.org/10.3390/w12030679.
70. Naghibi SA, Pourghasemi HR, Dixon B. GIS-based groundwater potential mapping using boosted regression tree, classification and regression tree, and random forest machine learning models in Iran. Environ Monit Assess. 2016;188(1):1–27. https://doi.org/10.1007/s10661-015-5049-6.
71. Yiran GAB, Kwang C, Blagogie L. Optimizing flood risk modelling with high-resolution remote sensing data and analytic hierarchy process. SN Soc Sci. 2024. https://doi.org/10.1007/s43545-024-00909-6.